A MODEL STUDY OF THE ROLE OF NONUNIFORM DEFECT DISTRIBUTION ON PLASTIC SHEAR LOCALIZATION

Y. Huang and J. W. Hutchinson

Division of Applied Sciences
Harvard University
Cambridge, MA 02138

Abstract

A model is introduced and analyzed for localization of plastic flow in anti-plane shear arising from strain softening material behavior. The model predicts the evolving shear strain variation in a band within which strain softening starts at "defects" which are distributed in various ways in the band. Results for a single defect, uniformly distributed defects, clustered defects, and nonuniformly distributed defects are presented and compared. A scheme for estimating the localization strain due to an arbitrary nonuniform distribution of defects based on the notion of a critical cluster is proposed and evaluated. The scheme has promise for extension to predict localization in the presence of actual distributions of voids or void-nucleating particles in ductile materials.

Ashby Symposium: The Modelling of
Material Behavior and Its Relation to Design
Edited by J.D. Embury and A.W. Thompson
The Minerals, Metals & Materials Society, 1990

1. Introduction

The predominant ductile failure mechanism in structural metals is micro-void nucleation, growth and coalescence. Flow localization is usually the critical step in the failure process in that the nucleation and growth of the voids results in strain softening which promotes instability in the form of a separation or shear band. Localization can be triggered by void nucleation, especially in high strength, low strain hardening materials. Moreover, localization can begin when the void fraction is still tiny (e.g. a small fraction of a percent) with coalescence occurring late in the process. The localization process itself is highly sensitive to nonuniformity in the distribution of voids or void-nucleating particles. This is most clearly seen from the infinite band calculations of Yamamoto (1) and Saje, Pan and Needleman (2), as illustrated for a separation band in Fig. 1.1. In these studies the material is characterized by Gurson's (4) continuum theory of dilatational plasticity. In the examples in Fig. 1.1 the

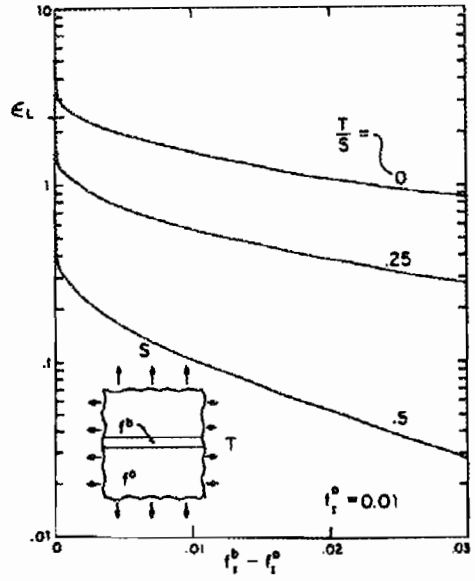

Fig. 1.1 Axisymmetric localization strain in infinite band with stress S normal to band and stress T tangent to band. The difference between initial void volume fraction in the band and outside the band is $f_f^b - f_f^0$. The strain hardening exponent is 1/10 --- see Ohno and Hutchinson (3) for further details.

material in the band has an initial void volume fraction, f^b, which is greater than that, f^0, for the material outside the band. The calculation tracks the deformation in the incipient band relative to that outside the band until localization starts wherein all subsequent plastic deformation takes place in the band. The figure shows how strongly the strain at the onset of localization (i.e. the

maximum strain obtained outside the band) depends on the nonuniformity of the void distribution as measured by $f^b - f^0$. Differences of void volume fraction between the material inside and outside the band of just 10^{-3} result in a substantial drop in ductility, particularly at high triaxiality T/S. The reference for $f^b = f^0$ is the material with a uniform distribution of voids. Then, localization occurs as a bifurcation-type instability.

While the infinite band studies reveal the highly imperfection-sensitive nature of the localization process, the infinite band imperfection is not a realistic nonuniformity. Nevertheless, Spitzig, Smelser and Richmond (5) showed that experimental trends for localization-limited ductility in iron compacts with initial porosity could be approximately reproduced using infinite band predictions if the initial band porosity was taken to be 1.5 to 2 times the average porosity. At the same time, their observations of the actual initial distribution of the voids revealed clusters of voids where the local porosity was as much as 4 to 7 times the average porosity.

Calculations for more realistic nonuniform distribution of voids or void-nucleating particles are extremely difficult due to the nonlinear character of void growth and interaction and of the localization process itself. We mention three such studies here, each of which considers material with an initial nonuniform distribution of voids. Ohno and Hutchinson (3) considered circular disc-shaped clusters normal to the direction of principal straining and leading to a separation band of the kind which occurs in the central region of the cup-cone of a tensile specimen. This study was introduced to answer the question of how large must the cluster be for it to be almost as deleterious as the infinite band nonuniformity. The curves in Fig. 1.2 show the relation between the localization strain and the size of the cluster for four

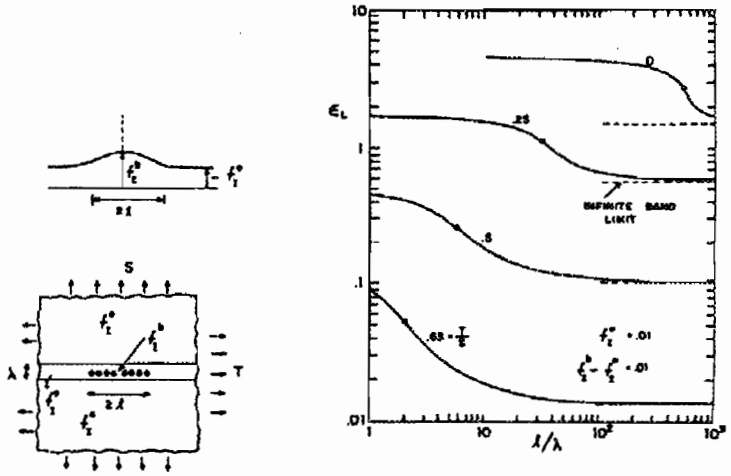

Fig. 1.2 Axisymmetric localization strain due to disk-shaped cluster of voids of width $\approx 2l$ and thickness λ. Material properties are otherwise the same as in Fig.1.1 --- see Ohno and Hutchinson (3) for further details.

triaxiality levels. For sufficient large cluster size the localization strain does approach the infinite band predictions of Fig. 1.1. In the limit as the cluster size goes to zero the bifurcation localization strain for the uniform distribution pertains. The size of the cluster corresponding to the transition between the two limits (designated by a dot in Fig. 1.2) is much smaller at high triaxiality than at low triaxiality. At low triaxiality large clusters are required to cause a significant loss in ductility due to nonuniformity. By contrast, at high stress triaxiality nonuniformity in the form of relatively small clusters are severely deleterious. One obvious conclusion to be drawn from these results is that one can not infer localization-limited ductility by considering the interaction between just a few neighboring voids, as has sometimes been attempted. Generally speaking, localization involves the collective interaction among a fairly large group of voids which then engulf even more voids.

Becker (6) has carried out a two-dimensional plane strain finite element study of localization using the Gurson's continuum material model where the distribution of the initial porosity was chosen in accord with a pattern measured in a two-dimensional section of a powdered iron compact. By comparing the macroscopic behavior of the material with the nonuniform distribution with that due to a uniform distribution with the same average initial void volume fraction, Becker established that prior to localization there was little observable influence of nonuniformity on macroscopic response. However, localization occurred in the material with the nonuniform distribution at much lower overall strain.

A series of model experiments by Magnusen, Dubensky and Koss (7) on thin strips pulled in tension was designed to illuminate the effect of nonuniform void distribution on strain to failure by localization. A group of specimens was prepared with circular holes of identical diameter and with the same number of holes per unit area. The centers of the holes were located randomly subject to a constraint on the distance between holes. The level of nonuniformity was varied by changing the minimum allowable distance between centers --- the smaller the minimum, the greater the nonuniformity in the distribution. The experimentally measured strain to localization dropped significantly as the nonuniformity in the distribution increased. The effects of nonuniformity are large with more than a factor of two reduction in the localization strain for the most nonuniform distributions compared to specimen with a uniform distribution of holes. A theoretical model which simulates the interaction between the nonuniformly distributed holes in the strips to predict the localization strain has been proposed by Magnusen, Srolovitz and Koss (8). As in the case of the model presented in this paper, their model was formulated with an eye to keeping the computational effort at a level such that results for many realizations of distributions could be generated.

The main aim of this paper is a study of the relation between strain localization and nonuniformity in the distribution of the microstructural defects which cause damage. A relatively simple anti-plane shear model is proposed which permits the calculation of the localization strain for any given distribution of defects. The model is used to identify a scheme

for characterizing nonuniformity and for predicting its effect on localization failure.

2. Model for Localization in Anti-plane Shear

The main features of the model are introduced in Fig. 2.1. The stress-strain curve of the material in pure shear is characterized by its elastic modulus μ, its linear hardening tangent

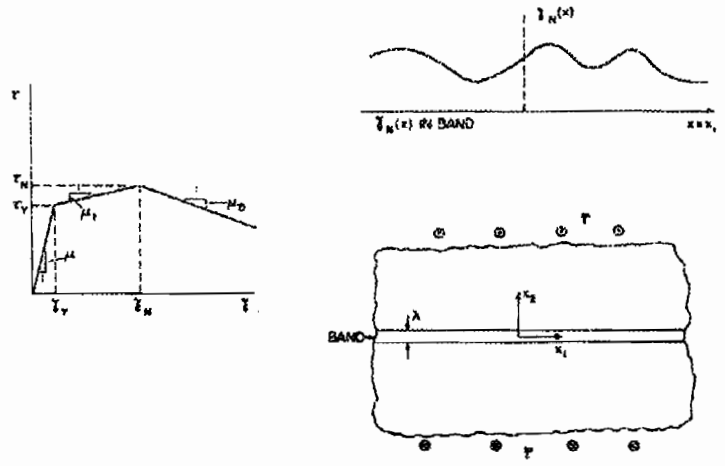

Fig.2.1 Details of anti-plane shear model: pure shear stress-strain curve on left; distribution of strain at onset of softening, $\gamma_N(x)$, in band at upper right; and shear band geometry at lower right.

modulus μ_t, and a softening modulus μ_D governing behavior once the nucleation of micro-voids starts at $\gamma = \gamma_N$. That is, in pure shear

$$\dot{\tau} = \begin{cases} \mu\dot{\gamma} & \gamma \le \gamma_Y \\ \mu_t\dot{\gamma} & \gamma_Y < \gamma \le \gamma_N \\ -\mu_D\dot{\gamma} & \gamma > \gamma_N \end{cases} \qquad (2.1)$$

Whether the continuing softening is due to deformation of the voids or continuous nucleation of additional micro-voids is not at issue here. It is assumed that the nucleation strain in the potential localization band is nonuniformly distributed according to $\gamma_N(x)$. The model is used to explore the spread of the softening regions, their interactions, and the ultimate shear localization in the band.

The infinite blocks of material on either side of the band are assumed to have a large nucleation strain so that nucleation, and therefore softening, is confined to the band. The

thickness of the band is taken to be λ. In an actual material λ is determined by the micro-structure and is typically on the order of the micro-void spacing. The following two modeling approximations are made:

(i) With $\tau_i \equiv \sigma_{3i}$ and $\gamma_i \equiv 2\varepsilon_{3i}$ $(i = 1,2)$ as the non-zero stresses and strains in anti-plane shear, the incremental stress-strain behavior according to J_2 flow theory for plastic loading in the hardening range is

$$\dot{\gamma}_i = \mu^{-1}\dot{\tau}_i + (\mu_t^{-1} - \mu^{-1})\tau_j\tau_k\dot{\tau}_k/(\tau_j\tau_j) \tag{2.2}$$

where a repeated indice implies summation. The incremental moduli in the infinite blocks of material on either side of the band are taken to be uniform and equal to values at infinity. That is, with $\tau_2 = \bar{\tau}$ and $\tau_1 = 0$ in (2.2), the incremental relation in the blocks for $\bar{\tau} > \tau_Y$ is

$$\dot{\gamma}_1 = \mu^{-1}\dot{\tau}_1 \quad , \quad \dot{\gamma}_2 = \mu_t^{-1}\dot{\tau}_2 \tag{2.3}$$

(ii) The strain in the band is taken to be independent of x_2. Because of the symmetry, $\gamma_1 = 0$ in the band. Thus the stress and strain in the band, $\tau(x) \equiv \tau_2(x)$ and $\gamma(x) \equiv \gamma_2(x)$, satisfy the pure shear relation shown in Fig. 2.1 and specified by (2.1).

This completes the specification of the model. The equations governing the distribution of τ and γ in the band can be reduced to an integral equation. For a given distribution of nucleation strain $\gamma_N(x)$, the integral equation is solved numerically at increasing levels of remote overall strain $\bar{\gamma}$ until localization occurs, as will be discussed in more detail below. The formulation of the governing equations for the various cases discussed below are given in the Appendix along with some discussion of the numerical solution methods.

3. Single Defect

The first distribution of nucleation strain in the band to be considered will be referred to as a single defect. Interaction between multiple defects will be considered in later sections. For the single defect (with $x \equiv x_1$)

$$\gamma_N(x) = \gamma_N^0 + (\gamma_N^* - \gamma_N^0)\exp\left[-\frac{1}{2}\left(\frac{x}{l}\right)^2\right] \tag{3.1}$$

As shown in Fig. 3.1, l is a measure of the half-width of the defect, γ_N^* is the minimum nucleation strain at the center of the defect, and γ_N^0 is the nucleation strain well away from the center. The level γ_N^0 can be regarded as the nucleation strain in the material outside the band as well since $\bar{\gamma}$ never exceeds γ_N^0 and thus nucleation is confined to the band, as already mentioned. In other words, the single defect case represents a local region of width of roughly $2l$ in which the nucleation strain has a minimum γ_N^* below the otherwise uniform level γ_N^0 of

the surrounding material.

As $\bar{\gamma}$ is increased from zero the behavior in the band and blocks is uniform until $\bar{\gamma}$ attains γ_N^* . For $\bar{\gamma} > \gamma_N^*$ the region of softening in the band spreads and the strain in the band in the vicinity of the defect grows more rapidly than the overall strain $\bar{\gamma}$. This is illustrated by a plot of the strain at the center of the defect versus $\bar{\gamma}$ in Fig. 3.2. The localization strain $\bar{\gamma}_L$ is

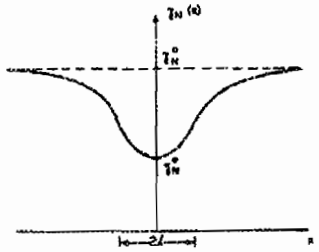

Fig.3.1 Distribution of $\gamma_N(x)$ corresponding to single defect.

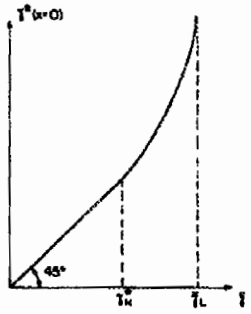

Fig.3.2 Behavior of shear band at center of defect versus remote strain showing the limit strain corresponding to localization.

precisely defined as the value of $\bar{\gamma}$ at which additional strain in the band can occur with no further increase in $\bar{\gamma}$. In effect, the softening region has grown large enough to cause nucleation, and thus softening, to spread with no further increase in remote stress $\bar{\tau}$.

Computed values of the localization strain $\bar{\gamma}_L$ as a function of γ_N^* for various sizes of defects, l/λ , are shown in Fig. 3.3 for the choice of model parameters

$$\mu_t = 0.05\mu \quad , \quad \mu_D = 0.01\mu \quad , \quad \gamma_N^0 = 15\gamma_Y \tag{3.2}$$

The following observations are evident from Fig. 3.3. For small defects with l/λ less than about 1, the defect has little effect on localization and $\bar{\gamma}_L \cong \gamma_N^0$. For large defects with l/λ

greater than about 10, localization sets in very soon after the first occurrence of nucleation and $\bar{\gamma}_L$ is only slightly larger than γ_N^*. For a given size of defect, l/λ, $\bar{\gamma}_L$ diminishes nearly (but not exactly) linearly with $\gamma_N^0 - \gamma_N^*$.

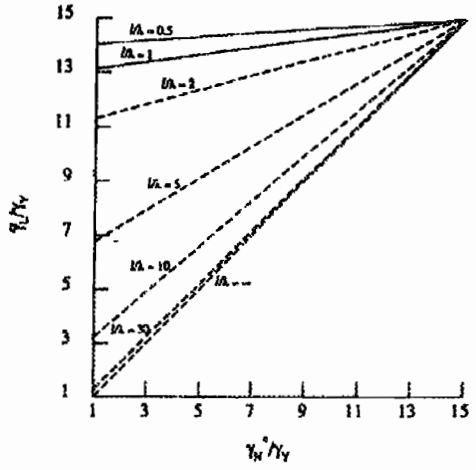

Fig. 3.3 Localization strain versus nucleation strain for single defect of various sizes, l/λ, of defects ($\mu_t = 0.05\mu$, $\mu_D = 0.01\mu$, $\gamma_N^0 = 15\gamma_Y$).

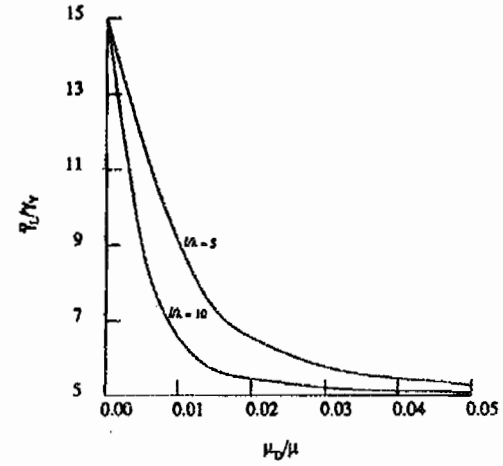

Fig. 3.4 Localization strain versus softening modulus for two sizes of single defects ($\mu_t = 0.05\mu$, $\gamma_N^0 = 15\gamma_Y$, $\gamma_N^* = 5\gamma_Y$).

The model also predicts a strong sensitivity of the localization strain to the softening modulus μ_D. Figure 3.4 displays this dependence for two sizes of defects with $\mu_t = 0.05\mu$, $\gamma_N^* = 5\gamma_Y$, and $\gamma_N^0 = 15\gamma_Y$. As an aside, we note that the source of continued softening in shear in a given material element is not at all well established. Continuing nucleation of micro-voids would produce continuing softening. Another mechanism proposed by Teirlinck, Zok, Embury and Ashby (9) involves finite deformation of existing voids without additional nucleation, but the status of this mechanism is still uncertain (10).

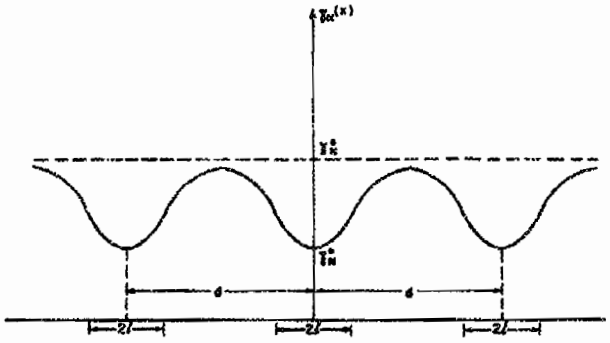

Fig. 4.1 Distribution of $\gamma_N(x)$ for uniformly distributed defects.

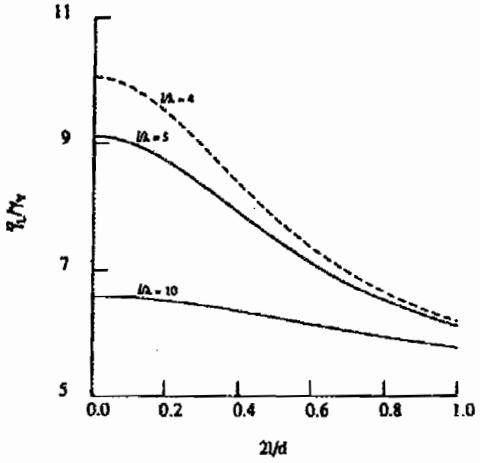

Fig. 4.2 Localization strain versus the ratio of defect size to defect spacing for uniformly distributed defects of various sizes ($\mu_t = 0.05\mu$, $\mu_D = 0.01\mu$, $\gamma_N^0 = 15\gamma_Y$, $\gamma_N^* = 5\gamma_Y$).

4. Uniformly Distributed Defects

Interaction among defects is now explored for a uniform distribution of defects. The distribution $\gamma_N(x)$ shown in Fig. 4.1 has period d with the centers of the defects located at $x_i = id$, $i = 0, \pm1, \pm2, \ldots$. Within each "defect" the nucleation strain varies in the same manner as in the single defect case, i.e.

$$\gamma_N(x) = \gamma_N^0 + (\gamma_N^* - \gamma_N^0) \exp\left[-\frac{1}{2}\left(\frac{x-x_i}{l}\right)^2\right] \qquad (4.1)$$

for $|x-x_i| \le d/2$.

The dependence of the localization strain on the size to spacing ratio of the defects, $2l/d$, is shown in Fig. 4.2 for three sizes of defects, l/λ . The parameters of the model used in these calculations are those in (3.2) with $\gamma_N^* = 5\gamma_Y$. For sufficiently widely spread defects (i.e. $2l/d < 0.1$ in Fig. 4.2) there is essentially no interaction and $\bar{\gamma}_L$ coincides with the single defect result as $2l/d \to 0$. However, when the spacing is decreased, interaction becomes pronounced reducing the localization strain well below the single defect result and ultimately to γ_N^* when the defects "overlap" significantly.

5. Clusters of Defects

We now consider nonuniform distributions in the form of clusters of defects. The cluster results will play a central role in a scheme proposed in the next section for estimating the localization strain for an arbitrarily nonuniform distribution of defects.

An n-defect cluster has n equally spaced defects with centers at

$$x_i = (i-1)d \qquad (i = 1,n) \qquad (5.1)$$

where the left-most defect is arbitrarily centered at $x_1 = 0$ and d is the spacing between centers. The distribution of the nucleation strain is still given by (4.1) for $|x-x_i| \le d/2$ with i = 2, n-1. For the left-most defect (i.e. $x < d/2$) γ_N is given by (4.1) with $x_i = 0$, where for the right-most defect (i.e. $x > (n-3/2)d$), γ_N is given by (4.1) with $x_i = (n-1)d$.

Curves of localization strain $\bar{\gamma}_L$ as a function of defect spacing d are shown in Fig. 5.1 for clusters of 2, 3, 4 and 5 defects. These curves are computed with the model parameters chosen to be

$$\mu_t = 0.05\mu \ , \ \mu_D = 0.01\mu \ , \ \gamma_N^0 = 1.5\gamma_Y \ , \ \gamma_N^* = 5\gamma_Y \ \text{ and } \ l/\lambda = 4 \qquad (5.2)$$

For large spacing d the interaction between the individual defects in the cluster becomes negligible and $\bar{\gamma}_L$ approaches the result for an isolated single defect. The closer the spacing, the greater the interaction and the smaller the localization strain. The lowest curve in Fig. 5.1

labeled n = ∞ is the result for the uniformly spaced periodic defect distribution of Section 4. Note that the 5-defect cluster is almost as deleterious as the infinite-defect distribution.

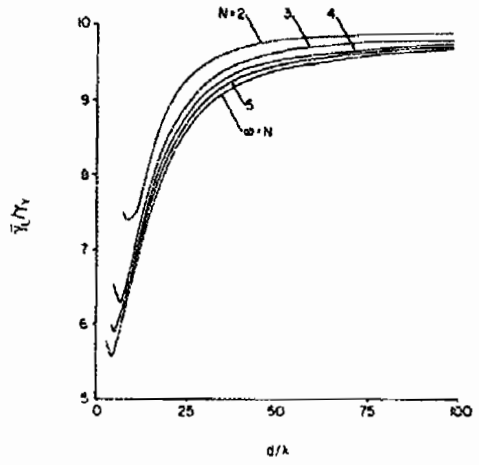

Fig. 5.1 Localization strain versus spacing between defects, d/λ, for clusters of defects ($N = 2, 3, 4, 5$ and ∞) ($\mu_t = 0.05\mu$, $\mu_D = 0.01\mu$, $\gamma_N^0 = 15\gamma_Y$, $\gamma_N^* = 5\gamma_Y$, $l/\lambda = 4$).

While the qualitative features predicted by this model are likely to have general validity, detailed predictions, such as the number of defects needed to constitute a deleterious cluster, are likely to be model specific. For example, the study of Ohno and Hutchinson (3) indicates that the size of a deleterious cluster in a separation localization is a strong function of stress triaxiality. Whether this is so in shear localization is not known.

6. Nonuniform Distributions of Defects and a Scheme for Estimating Localization Based on Cluster Data

Let $0 \le x \le L$ be a segment of the x-axis on which a representative distribution of defects exists (such as a typical section of a material element examined for defects). Suppose there are N defects each of width $2l$ within this segment. Outside this segment let the distribution of defects be periodic with period L. That is, the representative segment of x-axis is repeated over the whole x-axis. The area fraction, or line fraction, of defects is $2Nl/L$.

Let the centers of the defects, x_i ($i = 1, 2, \ldots, N$), within the representative segment [0,L] be randomly located. The nucleation strain $\gamma_N(x)$ within [0,L] is again determined by (4.1) where x_i is the center within [0,L] nearest x. For a given realization $\gamma_N(x)$ the localization

strain can be calculated numerically using the integral equation formulation given in the Appendix.

Four realizations are given in Table 1 chosen to emphasize the effect of clustering. These same realizations will be used to motivate a scheme for estimating the localization strain. Each of the four-defect distributions in Table 1 has the same line fraction of defects, $2Nl/L = 0.16$. The first is a uniform distribution which coincides with the case discussed in Section 4. The second, third and fourth distributions correspond to N = 4 but with two, three and four defects clustered together, respectively. The localization strains for these four distributions differ significantly, ranging from $9.52\gamma_Y$ for the uniform distribution to $5.78\gamma_Y$ for the 4-defect cluster. The effect of nonuniformity is clearly important with clustering promoting earlier localization.

Table 1. Four typical distributions with the same line fraction of defects show the significant difference of the localization strains, where x_i (i = 1,2,3,4) is the center of the defects.

$\mu_t = 0.05\mu$, $\mu_D = 0.01\mu$, $\gamma_N^0 = 15\gamma_Y$, $\gamma_N^* = 5\gamma_Y$, $l/\lambda = 4$, N = 4 and $L/\lambda = 200$

Distributions	x_1/λ	x_2/λ	x_3/λ	x_4/λ	$\tilde{\gamma}_L/\gamma_Y$
uniform defects	25	75	125	175	9.52
2 defect cluster	25	35	125	175	7.39
3 defect cluster	25	31	37	175	6.29
4 defect cluster	25	30.2	35.4	40.6	5.78

We can use these same four distributions to illustrate another nonlinear aspect of clustering. Define the average strain in the band as

$$\gamma_{ave} = L^{-1}\int_0^L \gamma(x)dx \tag{6.1}$$

Fig. 6.1 displays the remote shear stress (which necessarily coincides with the average stress in the band) as a function of γ_{ave} for each distribution. The overall strain in an actual specimen is the weighted average of the strain in the band and the strain outside the band. From Fig. 6.1 it is evident that the overall stress-strain curve will be lowered by clustering. This feature is observed in the stress-strain curves for the perforated strips measured by Magnusen, Dubensky and Koss (7).

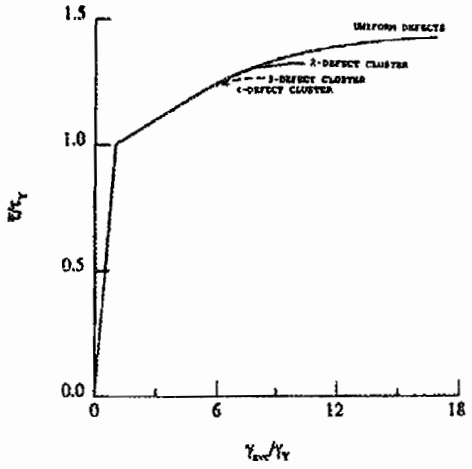

Fig. 6.1 Remote stress versus average strain in band for 4 defect distributions in Table 1. Each distribution has the same fraction of defects corresponding to 0.16.

Estimation Scheme

We now introduce the notion of a critical cluster to estimate the localization strain for a given nonuniform distribution of defects. With x_i (i = 1, N) as the defect centers within the representative section.

(1) Find the pair of defects closest to one another, denote the distance between their centers by $d^{(2)}$, and let $\gamma_L^{(2)}$ be the localization strain predicted for the 2-defect cluster with spacing $d = d^{(2)}$ in Fig. 5.1 (or from a similar plot with basic parameters μ, μ_t, μ_D, τ_Y, etc. corresponding to that of the material element).

(2) Similarly, for i = 3, 4, ... , find the smallest i-defect cluster, let $d^{(i)}$ denote the average spacing between the centers for the defects in the cluster, and let $\gamma_L^{(i)}$ denote the result from a plot like Fig. 5.1 for the localization of an i-defect cluster with spacing $d = d^{(i)}$.

(3) Identify the critical cluster as the one with the lowest localization strain, i.e.

$$\gamma_L^c = \min \left\{ \gamma_L^{(2)}, \gamma_L^{(3)}, \gamma_L^{(4)}, \ldots \right\} \tag{6.2}$$

(4) Take γ_L^c as the estimate of $\bar{\gamma}_L$.

Verification of the Estimate Scheme

This scheme was tested against the full integral equation solution for $\bar{\gamma}_L$ for more than 2000 distributions generated randomly. The parameters were chosen as $\mu_t = 0.05\mu$, $\mu_D = 0.01\mu$, $\gamma_N^0 = 15\gamma_Y$, $\gamma_N^* = 5\gamma_Y$ and $l/\lambda = 4$, and the centers of the defects were located by

a random number generator but were not permitted to be closer to one another than the defect half width, l. The error between the estimate, γ_L^e, and the computed localization strain $\bar{\gamma}_L$ never exceeded 3%, in any of the more than 2000 realizations.

The success of the estimation scheme reflects the fact that the nonlinear localization process is largely controlled by the most critical cluster of defects. In principle, the estimation scheme can be generalized to more complicated models and even to actual materials. However, the scheme does require that results for the effect of the basic n-defect clusters (such as those in Fig. 5.1) are available either from computation or experimentation.

Correlation of $\bar{\gamma}_L$ with the Minimum Spacing Between Defects

In their series of perforated thin strip experiments, Magnusen, Dubensky and Koss (7) found the localization strain to diminish with increasing nonuniformity as measured by the minimum spacing between holes. Motivated by this observation, we have taken the more than 2000 realizations for which $\bar{\gamma}_L$ was computed in the above subsection and have plotted $\bar{\gamma}_L$ as a function of the minimum spacing, d_{min}, occurring between any two defects for each realization. The upper and lower curves in Fig. 6.2 correspond to the envelopes of largest and smallest values of $\bar{\gamma}_L$ attained at a given d_{min}. The strong correlation of $\bar{\gamma}_L$ with d_{min} seen in the experiments of Magnusen *et al.* (7-8) also holds for the model. The lower curve in Fig. 6.2

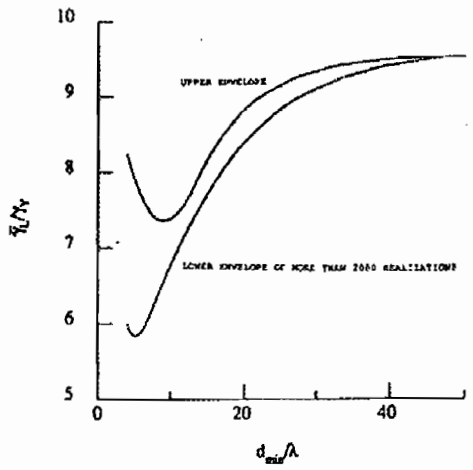

Fig. 6.2 Envelope of localization strain versus the minimum defect spacing for more than 2000 distributions ($\mu_1 = 0.05\mu$, $\mu_D = 0.01\mu$, $\gamma_N^0 = 15\gamma_Y$, $\gamma_N^* = 5\gamma_Y$, $l/\lambda = 4$, $N = 4$).

is quite close to the prediction for uniformly distributed defects where d_{min} is identified with d in Fig. 5.1. This is readily understood because $\bar{\gamma}_L$ for a large cluster approaches that for a uniform distribution with the same spacing (cf. Fig. 5.1). On the other hand the upper curve in Fig. 6.2 is very close to curve for the 2-defect cluster in Fig. 5.1. Again, this is readily understood in terms of the presence of a realization with an actual 2-defect cluster with $d_{min} = d$. The spread between the upper and lower curves in Fig. 6.2 obviously reflects the susceptibility of the material to the size of the actual cluster over and above the minimum spacing. At low minimum spacing the variability is fairly large in the case of the model and the correlation of $\bar{\gamma}_L$ with d_{min} is not as strong as at larger values of d_{min}.

Acknowledgement

The authors acknowledge many stimulating discussions related to the general subject area with O. Richmond. The estimation scheme discussed in Section 6 was an outgrowth of these discussions. This work was supported in part by the Materials Research Laboratory under Grant NSF-DMR-86-14003 and in part by the Division of Applied Sciences, Harvard University.

References

1. H. Yamamoto, "Conditions for shear localization in the ductile fracture of void-containing materials", Int. J. Fracture, 14 (1978) 347-365.

2. M. Saje, J. Pan and A. Needleman, "Void nucleation effects on shear localization in porous plastic solids", Int. J. Fracture, 19 (1982) 163-182.

3. N. Ohno and J. W. Hutchinson, "Plastic flow localization due to non-uniform void distribution", J. Mech. Phys. Solids, 32 (1984) 63-85.

4. A. L. Gurson, "Continuum theory of ductile rupture by void nucleation and growth: Part 1 - Yield criteria and flow rules for porous ductile media", J. Engng. Mat. Tech., 99 (1977) 2-15.

5. W. A. Spitzig, R. E. Smelser and O. Richmond, "The evolution of damage and fracture in iron compacts with various initial porosities", Acta Metall., 36 (1988), 1201-1211.

6. R. Becker, "The effect of porosity distribution on ductile failure", J. Mech. Phys. Solids, 35 (1987) 577-599.

7. P. E. Magnusen, E. M. Dubensky and D. A. Koss, "The effect of void arrays on void linking during ductile fracture", Acta Metall., 36 (1988) 1503-1509.

8. P. E. Magnusen, D. J. Srolovitz and D. A. Koss, "A simulation of void linking during ductile fracture", to be published.

9. D. Teirlinck, F. Zok, J. D. Embury and M. F. Ashby, "Fracture mechanism maps in stress space", Acta Metall.,36 (1988) 1213-1228.

10. N. A. Fleck, J. W. Hutchinson and V. Tvergaard, "Softening by void nucleation and growth in tension and shear", Report MECH-123, Division of Applied Sciences, Harvard University, to be published in J. Mech. Phys. Solids.

APPENDIX

Governing Equations

Single Defect

The integral equation governing the shear stress distribution within the band is now specified. Nucleation always occurs after the two blocks on either side of the band have yielded. Write the total displacement as

$$u_3 = \bar{\gamma} x_3 + w(x_1, x_2) \tag{A.1}$$

with w denoting the contribution additional to the displacement associated with the uniform state. With $\bar{\gamma}$ increased monotonically above γ_Y and with uniform moduli in the blocks associated with the stress state at infinity, J_2 flow theory can be "integrated-up" to give the following equation for w

$$\mu w_{,11} + \mu_t w_{,22} = 0 \tag{A.2}$$

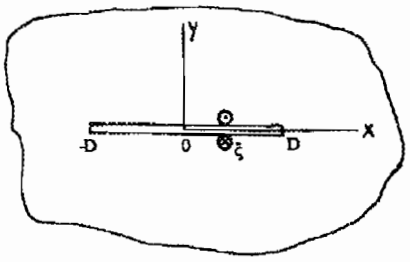

Fig. A.1

The equation governing the distribution of $\tau_{32} \equiv \tau(x)$ within the portion of the band wherein nucleation has occurred is formulating by taking the stress and shear displacement across the band as the boundary conditions on a "crack", in analog to the Dugdale-Barenblatt model. Denote the segment of the band in which nucleation has occurred (i.e. $\gamma > \gamma_N(x)$) by $|x| < D$. Let $K(x,\xi)$ be the crack opening displacement at x due to a pair of "wedging" forces on the otherwise traction free crack faces at ξ as shown in Fig. A.1. By solving (A.2) with appropriate boundary conditions, one finds

$$K(x,\xi) = \frac{2}{\pi\sqrt{\mu\mu_t}} \log\left[\frac{D|x-\xi|}{D^2 - x\xi + \sqrt{D^2-x^2}\sqrt{D^2-\xi^2}}\right] \tag{A.3}$$

The extra shearing displacement $\delta(x) = w(x,0+)-w(x,0-)$ of one crack face relating to another for $|x| < D$ is given by

$$\delta(x) = \int_{-D}^{D} K(x,\xi)\tau(\xi)d\xi + 2\bar{\tau}(\mu\mu_t)^{-1/2}\sqrt{D^2-x^2} \qquad (A.4)$$

where the second term is the opening due to the remote stress $\bar{\tau}$. The extra shearing displacement is taken to be related to the shear strain in the band, $\gamma(x)$, by

$$\delta(x) = \lambda[\gamma(x) - \hat{\gamma}(\tau(x))] \qquad (A.5)$$

where $\hat{\gamma}(\tau)$ is the strain at stress τ had nucleation not occurred, i.e.

$$\begin{aligned} \hat{\gamma}(\tau) &= \mu^{-1}\tau \qquad && \text{for } \tau \le \tau_Y \\ &= \gamma_Y + \mu_t^{-1}(\tau-\tau_Y) && \text{for } \tau \ge \tau_Y \end{aligned} \qquad (A.6)$$

Equation (A.4) thus models the additional strain in the band as measured by $\delta(x)$ due to nucleation of damage. It is an integral equation for $\tau(x)$, or equivalently for $\gamma(x)$, for $|x| \le D$. The equation must be supplemented by a condition which eliminates the singularity in τ at $x = \pm D$ and ensures that τ varies continuously across the ends of the nucleation region. This equation for D is

$$\frac{2}{\pi}\int_0^D \tau(\xi)\left(D^2-\xi^2\right)^{-1/2} d\xi = \bar{\tau} \qquad (A.7)$$

where the symmetry of shear stress τ, $\tau(-\xi) = \tau(\xi)$, has been used. As discussed in the body of the paper, the equation admits a solution for $\bar{\gamma} < \bar{\gamma}_L$. As $\bar{\gamma} \to \bar{\gamma}_L$, $d\gamma/d\bar{\gamma}_L$ grows without bound.

Uniformly Distributed Defects

The formulation for the periodic array of identical defects is similar to that just described. The kernel function for an array of cracks of period d is now

$$K(x,\xi) = \frac{2}{\pi\sqrt{\mu\mu_t}}\log\left\{\frac{f(D)|f(x) - f(\xi)|}{\cos\left(\frac{\pi\xi}{d}\right)\left[f(x) - f(D)\right]^{1/2} + \cos\left(\frac{\pi x}{d}\right)\left[f(\xi) - f(D)\right]^{1/2}}\right\} \qquad (A.8)$$

where $f(\zeta) \equiv \cos^2(\pi\zeta/d)$. The integral equation again takes the form (A.4) with (A.5) where now the second term on the right hand side of (A.4) is

$$\frac{2\bar{\tau}d}{\pi\sqrt{\mu\mu_t}}\log\left[\sqrt{\frac{f(x)}{f(D)}}+\sqrt{\frac{f(x)}{f(D)}-1}\right] \tag{A.9}$$

Equation (A.7) is replaced by

$$2d^{-1}\int_0^D \tau(\xi)\left\{1-\left[\frac{f(D)}{f(\xi)}\right]\right\}^{-1/2} d\xi = \bar{\tau} \tag{A.10}$$

Nonuniform Distribution of Defects

The formulation of the model for clusters of defects and for arbitrarily nonuniform distributions differs from that described above in that it is incremental and it models the band somewhat differently. The incremental form of (A.2) governing the additional displacement increment $\dot{w}(x,y)$ in the blocks on either side of the band is

$$\mu\dot{w}_{,xx} + \mu_t\dot{w}_{,yy} = 0 \tag{A.11}$$

To couple the band to the blocks we will use the Green's function correspond to the displacement increment at (x,0) due to a unit concentrated shear load at (ξ,0) on an otherwise traction-free surface on y = 0 :

$$K(x,\xi) = \frac{1}{\pi\sqrt{\mu\mu_t}}\log|x-\xi| \tag{A.12}$$

The additional displacement increment $\dot{\delta}(x)$ across the band is now taken as

$$\dot{\delta}(x) = \lambda\left[\dot{\gamma}(x) - \dot{\bar{\gamma}}\right] \tag{A.13}$$

where γ is again the strain in the band and $\bar{\gamma}$ is the remote strain. The band and the blocks are coupled together using (A.12) by requiring that the additional displacement across the band be compatible with the additional displacement of the blocks, i.e.

$$\frac{1}{2}\dot{\delta}(x) = \int_{-\infty}^{\infty} K(x,\xi)\left[\dot{\tau}(\xi) - \dot{\bar{\tau}}\right]d\xi \tag{A.14}$$

For numerical purpose it is better to work with a modified form of (A.14):

$$\frac{1}{2}\left[\dot{\delta}(x) - \dot{\delta}(0)\right] = \int_{-\infty}^{\infty} \hat{K}(x,\xi)\left[\dot{\tau}(\xi) - \dot{\tau}(0)\right]d\xi \tag{A.15}$$

where $\hat{K}(x,\xi) = K(x,\xi) - K(0,\xi)$. The system of equations is completed by requiring $\dot{\gamma}$ and $\dot{\tau}$ to be related by (2.1) and by the overall equilibrium condition

(A.9)

$$\int_{-\infty}^{\infty}\left[t(\xi)-\dot{\bar{t}}\right]d\xi = 0 \tag{A.16}$$

Eqs. (4.15), (2.1), (A.13) and (A.16) comprise the set of incremental equations governing the increment of strain distribution in the band as a function of $\dot{\bar{\gamma}}$. Localization occurs when a non-zero distribution $\dot{\gamma}(x)$ is possible with $\dot{\bar{\gamma}} = 0$. As mentioned in Section 6, the nonuniform distribution was taken to be periodic with period L characterizing a representative material element. In this way the infinite integrals could be reduced to a sum of finite integrals of the form

(A.10)

$$\int_{-\infty}^{\infty}\hat{K}(x,\xi)f(\xi)d\xi = \sum_{j=-\infty}^{\infty}\int_{0}^{L}\hat{K}(x,jL+\zeta)f(\zeta)d\zeta \tag{A.17}$$

where f has period L . The sum was approximated by 201 terms with j summing from -100 to 100. This same procedure was applied to obtain the cluster results in Section 5. The length L was taken to be very large compared to total width of the cluster so that to a very good approximation the interaction between clusters was negligible.

nonuniform
lels the band
lisplacement

(A.11)

ipond to the
an otherwise

The model for the nonuniform distribution does not reduce exactly to the model for the single defect or the uniform distribution of defects when specialized to these cases. Nevertheless, the numerical predictions of the two models are very close when applied to the same defect distribution assuming λ/L is sufficiently small. For example, the results for the uniform distribution of defects in Fig. 4.2 are reproduced to within 0.5% by the general model as long as $\lambda/L \leq 0.005$.

(A.12)

(A.13)

the blocks are
ss the band be

(A.14)

(A.15)

iiring $\dot{\gamma}$ and $\dot{t}$